THE JOURNAL OF BIOLOGICAL CHEMISTRY
Vol. 273, No. 1, Issue of January 2, pp. 66–72, 1998

Printed in U.S.A.

Specificity of Mouse G_{M2} Activator Protein and β-*N*-Acetylhexosaminidases A and B

SIMILARITIES AND DIFFERENCES WITH THEIR HUMAN COUNTERPARTS IN THE CATABOLISM OF G_{M2}*

(Received for publication, August 21, 1997, and in revised form, October 21, 1997)

Jeffrey A. Yuziuk‡, Carmen Bertoni‡§, Tommaso Beccari§, Aldo Orlacchio§, Yan-Yun Wu‡, Su-Chen Li‡, and Yu-Teh Li‡¶

From the ‡Department of Biochemistry, Tulane University School of Medicine, New Orleans, Louisiana 70112 and §Dipartimento di Biologia Cellulare e Molecolare, Universita degli Studi di Perugia, Via del Giochetto, 06126 Perugia, Italy

Tay-Sachs disease, an inborn lysosomal disease featuring a buildup of G_{M2} in the brain, is caused by a deficiency of β-hexosaminidase A (Hex A) or G_{M2} activator. Of the two human lysosomal Hex isozymes, only Hex A, not Hex B, cleaves G_{M2} in the presence of G_{M2} activator. In contrast, mouse Hex B has been reported to be more active than Hex A in cleaving G_{M2} (Burg, J., Banerjee, A., Conzelmann, E., and Sandhoff, K. (1983) *Hoppe Seyler's Z. Physiol. Chem.* 364, 821–829). In two independent studies, mice with the targeted disruption of the *Hexa* gene did not display the severe buildup of brain G_{M2} or the concomitant abnormal behavioral manifestations seen in human Tay-Sachs patients. The results of these two studies were suggested to be attributed to the reported G_{M2} degrading activity of mouse Hex B. To clarify the specificity of mouse Hex A and Hex B and to better understand the observed results of the mouse model of Tay-Sachs disease, we have purified mouse liver Hex A and Hex B and also prepared the recombinant mouse G_{M2} activator. Contrary to the findings of Burg *et al.*, we found that the specificities of mouse Hex A and Hex B toward the catabolism of G_{M2} were not different from the corresponding human Hex isozymes. Mouse Hex A, but not Hex B, hydrolyzes G_{M2} in the presence of G_{M2} activator, whereas G_{M2} is refractory to mouse Hex B with or without G_{M2} activator. Importantly, we found that, in contrast to human G_{M2} activator, mouse G_{M2} activator could effectively stimulate the hydrolysis of G_{A2} by mouse Hex A and to a much lesser extent also by Hex B. These results provide clear evidence on the existence of an alternative pathway for G_{M2} catabolism in mice by converting G_{M2} to G_{A2} and subsequently to lactosylceramide. They also provide the explanation for the lack of excessive G_{M2} accumulation in the *Hexa* gene-disrupted mice.

Human tissues contain two major isoforms of lysosomal β-hexosaminidase (Hex),[1] Hex A, a heterodimeric protein composed of α- and β-subunits, and Hex B, a β-subunit homodimer (1, 2). These two isoforms have also been reported to exist in other mammals (3). Human Hex A hydrolyzes the GalNAc from G_{M2} in the presence of a specific protein cofactor, G_{M2} activator (4–6). Human Hex B, on the other hand, is not able to hydrolyze G_{M2} with or without G_{M2} activator (7–10). A deficiency of Hex A or G_{M2} activator causes Tay-Sachs disease in humans, a lysosomal storage disease characterized by an excessive buildup of G_{M2} in the central nervous system (11). Burg *et al.* (3) reported that, in sharp contrast to human Hex isozymes, the partially purified Hex B prepared from several different mammalian tissues were able to degrade G_{M2} and that rat Hex B degraded G_{M2} more effectively than the Hex A. They also reported that the mouse activator preparation made from heat-treated mouse kidney extract was only slightly effective in stimulating the hydrolysis of G_{M2} by mouse Hex A and inhibited mouse Hex B in the same reaction. Recently, in two independent studies, mice with the targeted disruption of the *Hexa* gene were found to display neither the severe buildup of brain G_{M2} nor the concomitant abnormal behavioral manifestations seen in human classical Tay-Sachs patients (12, 13). In both studies, the mild manifestations were attributed to the reported G_{M2} degrading activity of mouse Hex B (3). Based on the fate of the radioactive G_{M1} fed to embryonic fibroblasts derived from *Hexa* −/− and *Hexb* −/− mice, Sango *et al.* (14) proposed the presence of an alternative pathway in mice where sialidase acts upon G_{M2} to produce G_{A2} which can be hydrolyzed subsequently by Hex A or Hex B.

To clarify the role of the mouse Hex A and Hex B in the catabolism of G_{M2} and also to understand better the observed results of the mouse models of classical Tay-Sachs disease (Type B G_{M2} gangliosidosis), we have purified mouse liver Hex A and Hex B. We have also prepared the recombinant mouse G_{M2} activator. Using the recombinant human and mouse G_{M2} activators, we have studied the requirement of these two protein cofactors in the hydrolysis of G_{M2} and G_{A2} by mouse Hex A and Hex B. We have also studied the cross-reactivity of human and mouse G_{M2} activators by studying the stimulation of mouse Hex A by human G_{M2} activator and of human Hex A by mouse G_{M2} activator.

EXPERIMENTAL PROCEDURES

Materials—G_{M2} was isolated from the brain of a Tay-Sachs patient (15). G_{A2} was prepared from G_{M2} by mild acid hydrolysis (16).

* This work was supported by National Institutes of Health Grant NS 09626. The costs of publication of this article were defrayed in part by the payment of page charges. This article must therefore be hereby marked "*advertisement*" in accordance with 18 U.S.C. Section 1734 solely to indicate this fact.

¶ To whom correspondence should be addressed: Department of Biochemistry SL 43, Tulane University School of Medicine, 1430 Tulane Avenue, New Orleans, LA 70112. Tel.: 504-584-2459; Fax: 504-584-2739; E-mail: yli@tmcpop.tmc.tulane.edu.

[1] The abbreviations used are: Hex, β-*N*-acetylhexosaminidase; MU, 4-methylumbelliferyl; MUG, 4-methylumbelliferyl-β-GlcNAc; MUGS, 4-methylumbelliferyl-β-GlcNAc-6-SO_4; G_{M1}, Galβ1→3GalNAcβ1→4(NeuAcα2→3)Galβ1→4Glcβ1–1′Cer; G_{M2}, GalNAcβ1→4(NeuAcα2→3)Galβ1→4Glcβ1–1′Cer; G_{A2}, GalNAcβ1→4Galβ1→4Glcβ1–1′Cer; G_{M3}, NeuAcα2→3Galβ1→4Glcβ1–1′Cer; $II^3NeuAcGgOse_3$, the oligosaccharide derived from G_{M2}; FPLC, fast protein liquid chromatography; SP, sulfopropyl; PAGE, polyacrylamide gel electrophoresis.

$II^3NeuAcGgOse_3$ was prepared from G_{M2} using ceramide glycanase (17). Goat anti-human Hex A was a kind gift of Dr. Richard L. Proia, Section of Biochemical Genetics, Genetics and Biochemistry Branch, NIDDK, National Institutes of Health, Bethesda, MD. The following were purchased from commercial sources: frozen mouse livers (Swiss-Webster strain), Pel-Freez; precoated Silica Gel 60 thin layer chromatography plates, Fractogel EMD DEAE-650(M) and Fractogel SP-650(S), Merck (Darmstadt, Germany); protein standards for molecular weight and pI, FPLC Superose 6 and Mono P columns, Sephacryl S-300-SF, Polybuffer 74, Pharmacia Biotech Inc.; phenylmethylsulfonyl fluoride, Pierce; peroxidase-conjugated rabbit anti-goat IgG, 4-chloro-1-naphthol, MUG, Coomassie Brilliant Blue R-250, Trizma base, glycine, Sigma; MUGS, Research Development Corp., Toronto, Canada; Centricon-10 (10,000 molecular weight cutoff) micro-concentrators, Amicon.

Expression of Murine G_{M2} Activator—A pBluescript vector containing a 1.1-kilobase cDNA encoding the mouse G_{M2} activator (18) was used as a template to generate by polymerase chain reaction a shortened version of the encoding sequence which was homologous to the mature human G_{M2} activator (19). The upstream primer was 5′-ATG-ATG-GAT-CCG-GTG-GCT-TCT-CCT-GGG-ATA-3′ and the downstream primer was 5′-CAG-GCA-AGC-TTG-CTG-CTG-CCA-GGT-TAT-CTG-3′. This cDNA segment was subcloned into the pT7–7 expression vector at *Bam*HI and *Hin*dIII sites, and its sequence was verified to contain the 486-base-pair DNA fragment corresponding to amino acids 32–193 of the mouse G_{M2} activator (18). The recombinant mouse G_{M2} activator was expressed and purified according to the procedures described previously for the human G_{M2} activator (19). The NH_2-terminal amino acid sequence of the purified mouse G_{M2} activator was confirmed by a pulse-liquid protein micro-sequencer equipped with an on-line microbore phenylthiohydantoin-derivative analyzer (Applied BioSystems).

Enzyme Assays—Enzyme activity was determined by using fluorogenic substrates MUG and MUGS according to Potier *et al.* (20). The enzyme was incubated with 1.5 mM of substrate in 50 mM sodium citrate buffer, pH 5.0, in a total volume of 50 μl at 37 °C. After a set time, 1.5 ml of 0.2 M sodium borate buffer, pH 9.8, was added to the reaction mixture to stop the reaction. The released MU was determined using a Sequoia-Turner Model 450 fluorometer. One unit of enzyme activity is defined as the amount that liberates 1 μmol of MU/min at 37 °C. For glycolipid substrates G_{M2} and G_{A2}, the reaction mixture contained 3 nmol of substrate in 40 μl of 10 mM sodium acetate buffer, pH 5.0. The reactions were stopped by adding 40 μl of ethanol, and the mixtures were dried under vacuum, redissolved in 20 μl of chloroform/methanol (2:1, v/v), and applied onto a thin layer chromatography plate. The plates were developed by chloroform/methanol/water (60:35:8, v/v/v), sprayed with diphenylamine reagent (21), and heated at 115 °C for 15 min to visualize glycoconjugates.

Kinetic Analysis—Initial rate measurements and determination of kinetic parameters for the enzyme-catalyzed hydrolysis of synthetic substrates were conducted similarly to that described previously (22). The reactions were carried out in 20 mM sodium citrate buffer, pH 5.0, using 0–5.0 mM of the substrates MUG and MUGS.

Isoelectric Point Determination—Purified mouse liver Hex A and Hex B were examined by FPLC chromatofocusing in a pH range of 7.4–3.8 using a Mono P HR 5/20 (0.5 × 20 cm) column. The starting buffer was 25 mM imidazole-HCl, pH 7.4, and the running buffer was Polybuffer 74 adjusted to pH 3.8 using HCl as described in the Pharmacia manual. After applying the sample onto the Mono P column, the column was eluted with the running buffer at 0.5 ml/min and 0.5-ml fractions were collected.

Molecular Mass Determination—The molecular masses of purified mouse Hex A and Hex B were determined using Superose 6 FPLC gel filtration in 50 mM sodium phosphate buffer, pH 7.0, containing 0.15 M NaCl. The column was first calibrated under the same conditions using ferritin (440,000), catalase (232,000), aldolase (158,000), ovalbumin (49,500), and chymotrypsinogen A (25,000) as molecular weight standards.

Purification of Mouse Liver Hex A and Hex B—All operations were performed at 0–5 °C except the chromatographies on Con A-Sepharose and SP-Fractogel that were carried out at room temperature. Centrifugation was routinely carried out at 30,000 × *g* for 50 min using a Sorvall RC5C refrigerated centrifuge. Unless otherwise indicated, ultrafiltration was carried out with an Amicon stirred cell using a PM-10 membrane. Two hundred frozen mouse livers (391 g) were homogenized using a Polytron (Brinkmann) homogenizer with 5 volumes of cold phosphate-buffered saline (10 mM sodium phosphate, 138 mM NaCl, 2.7 mM KCl, pH 7.4) containing 1 mM EDTA and 1 mM phenylmethylsulfonyl fluoride as protease inhibitors, followed by centrifugation. The supernatant was brought to 30% saturation with solid ammonium sulfate. After 2 h, the precipitate was removed by centrifugation, and the supernatant was further brought to 65% saturation with solid ammonium sulfate. After standing overnight, the precipitate was collected by centrifugation and resuspended in 500 ml of 10 mM sodium phosphate buffer, pH 7.0 (buffer A). The suspension was placed into several dialysis bags and dialyzed against 10 liters of buffer A overnight, changing buffer every 4 h (4 changes). This crude enzyme preparation (780 ml) was centrifuged and applied to a DEAE-Fractogel column (5 × 45 cm) equilibrated with buffer A. The column was washed overnight with buffer A at 2 ml/min, and proteins were eluted with a linear gradient of NaCl from 0 to 0.5 M in the same buffer (total volume 4 liters), and 20-ml fractions were collected. Fractions were assayed for both MUG- and MUGS-cleaving activities. Hex B, which cleaves only MUG, was eluted in the nonadsorbed fractions (Fig. 1) and was concentrated by ultrafiltration. As shown in Fig. 1, MUG-cleaving activity eluted with NaCl as a main peak with a leading shoulder. The shoulder contained very low MUGS-cleaving activity, whereas the main peak contained both MUG- and MUGS-cleaving activities. Fractions in the main peak were pooled and concentrated to make a crude mouse Hex A preparation. This preparation was applied to a Sephacryl S-300 column (5 × 90 cm) equilibrated with 50 mM sodium phosphate buffer, pH 7.0, containing 0.15 M NaCl. The column was eluted with the same buffer at 1 ml/min, and 20-ml fractions were collected. MUG- and MUGS-cleaving activities coeluted as a broad peak, and the entire peak was pooled (Fig. 2*A*) and concentrated to 25 ml by ultrafiltration. The concentrated Hex A was dialyzed thoroughly against buffer A overnight. The crude Hex B preparation (from DEAE-Fractogel column) was dialyzed against buffer A and applied to an SP-Fractogel column (2.5 × 17 cm) equilibrated with buffer A. The column was washed with buffer A at 2 ml/min and eluted with a linear gradient of NaCl from 0 to 0.5 M in buffer A (total volume, 500 ml) and 17-ml fractions were collected. Fractions were assayed for MUG-cleaving activity. No activity was detected in the nonadsorbed fractions. The Hex B activity eluted as a single peak starting at 0.1 M NaCl was pooled and concentrated to make an SP-Fractogel-purified mouse Hex B preparation (elution pattern not shown). This preparation was applied to a Sephacryl S-300 column and eluted under the same conditions as the DEAE-Fractogel purified Hex A (Fig. 2*B*).

The dialyzed mouse Hex A after gel filtration was applied to a Con A-Sepharose column (2.5 × 33 cm) equilibrated with buffer A. The column was washed with buffer A at 2 ml/min, followed by buffer A containing 0.5 M NaCl and 17-ml fractions were collected. After the absorbance at 280 nm fell to a stable base line, the column was eluted with buffer A containing 0.5 M NaCl and 0.75 M methyl-α-mannoside. No MUG-cleaving activity was detected in the nonadsorbed or 0.5 M NaCl eluted fractions. The fractions eluted by methyl-α-mannoside contained MUG-cleaving activity (elution pattern not shown) and were

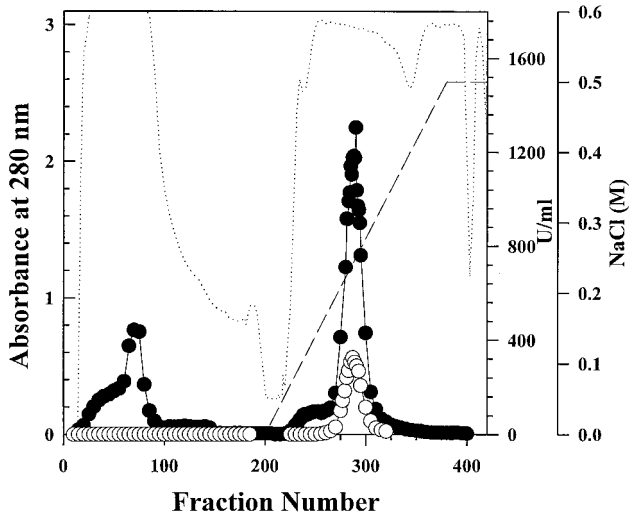

FIG. 1. **DEAE-Fractogel chromatography of mouse liver crude enzyme preparation.** Mouse liver crude enzyme preparation obtained after ammonium sulfate precipitation was applied onto a DEAE-Fractogel column (5 × 45 cm). Detailed conditions are described under "Experimental Procedures." *Dotted line*, absorbance at 280 nm; *filled circles*, MUG-cleaving activity; *empty circles*, MUGS-cleaving activity; *dashed line*, NaCl gradient.

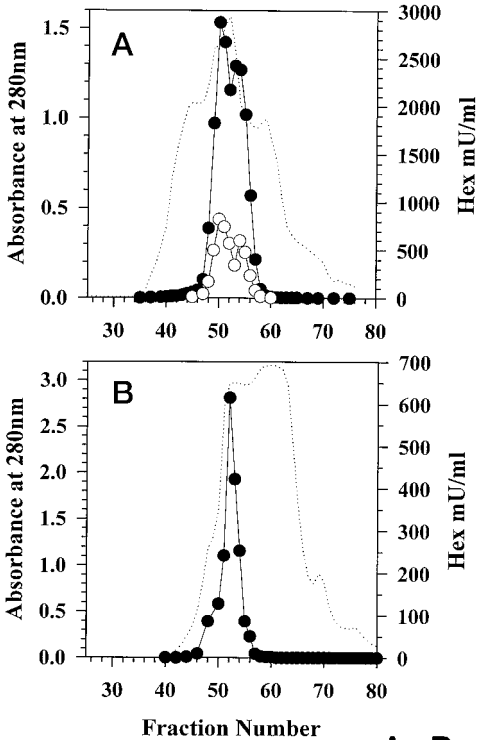

FIG. 2. **Sephacryl S-300 gel filtration chromatography of mouse Hex A (*A*) and Hex B (*B*).** Mouse DEAE-Fractogel purified Hex A and SP-Fractogel purified Hex B enzyme preparations were applied onto a Sephacryl S-300 column (5 × 90 cm). Detailed conditions are described under "Experimental Procedures." *Dotted line*, absorbance at 280 nm; *filled circles*, MUG-cleaving activity; *empty circles*, MUGS-cleaving activity.

pooled and concentrated to 7 ml and dialyzed against buffer A. The mouse Hex B preparation after Sephacryl S-300 gel filtration was also applied to a Con A-Sepharose column and processed in the same manner as the Hex A. Hex B also adsorbed to the column and was specifically eluted using buffer A containing 0.5 M NaCl and 0.75 M methyl-α-mannoside. Hex B after the Con A-Sepharose step was purified about 1000-fold and was used for subsequent experiments.

The dialyzed mouse Hex A preparation obtained after the Con A-Sepharose step was centrifuged and applied to an SP-Fractogel column (0.5 × 2 cm) equilibrated with buffer A (Fig. 3). The column was washed with buffer A at 0.5 ml/min and eluted with a linear NaCl gradient from 0 to 0.5 M in buffer A (total volume 40 ml) and 0.5-ml fractions were collected. Fractions were assayed for both MUG- and MUGS-cleaving activities. As shown in Fig. 3, the nonadsorbed fractions contained the majority of the protein with about one-third of the enzyme activity. The MUG- and MUGS-cleaving activities coeluted as a complex peak beginning at about 0.15 M NaCl and was partially resolved from the main UV-absorbing material. When Hex A-containing fractions were analyzed by SDS-PAGE under nonreducing conditions, fractions 116–132 (Fig. 3) were found to contain only one major protein band and were pooled and concentrated. By the above procedure, Hex A was purified about 1500-fold from the crude enzyme preparation and was used for subsequent studies. Table I summarizes the recovery of Hex A and Hex B from 200 mouse livers according to this purification scheme.

Western Blotting—The purified mouse liver Hex A after SP-Fractogel chromatography was analyzed by 15% SDS-PAGE (23). The gel was electrophoretically transferred onto a nitrocellulose membrane in 20 mM Tris/150 mM glycine buffer, pH 8.0, containing 20% methanol at 18 V for 4 h using a Bio-Rad transfer apparatus. Membranes were overlaid with goat anti-human Hex A (24, 25) as the primary antibody followed by horseradish peroxidase-conjugated rabbit anti-goat IgG as the secondary antibody. For visualization, the membrane was incubated with 8 mmol of 4-chloro-1-naphthol with 0.01% hydrogen peroxide to produce a purple color. The reaction was stopped by washing the membrane with water.

RESULTS

Purification and Characterization of Mouse Liver Hex A and Hex B—The two major Hex isozymes were resolved from the crude mouse liver extract by DEAE-Fractogel chromatography at pH 7.0 (Fig. 1). The acidic mouse Hex A was purified to near homogeneity using the scheme described under "Experimental Procedures" as summarized in Table I. The Hex A after SP-Fractogel chromatography was used for the subsequent studies. By SDS-PAGE under nonreducing conditions, the purified Hex A showed one broad protein band when stained by Coomassie Brilliant Blue (Fig. 4*A*, *lane 3*). Immunostaining with anti-human Hex A revealed two overlapping bands of equal intensity corresponding to molecular sizes of approximately 57 and 59 kDa (Fig. 4*B, lane 3*). This is in agreement with the postulated makeup of mouse Hex A, which is a heterodimer consisting of an α-subunit and a β-subunit, with molecular sizes before posttranslational processing of 60 and 61 kDa, respectively, as deduced from their cDNA sequences (26–28). In humans, the β-subunit is posttranslationally processed to form two smaller polypeptides, β1 and β2, which are joined by disulfide bonds (29). Fig. 4*A*, *lane 2,* shows that similar processing occurs in mouse Hex A, with the appearance under reducing conditions of two overlapping bands of about 27 and 24 kDa, and the concomitant disappearance of the 59-kDa band. Western blot analysis was used to confirm that the protein band visualized by Coomassie Brilliant Blue staining was indeed Hex A. Goat anti-human Hex A recognized both the nonreduced mouse Hex α- and β-subunits and the lower molecular size polypeptide chains after reduction (Fig. 4*B*). The native molecular sizes of the mouse Hex A and Hex B were determined to be 110 and 120 kDa, respectively, as estimated using Superose 6 FPLC gel filtration. These values suggest that the native structures of mouse Hex A and Hex B consist of dimers as is the case for human enzymes. The isoelectric points of the two isoforms were estimated using Mono P FPLC chromatofocusing to be 5.4–3.8 for the purified mouse Hex A and 6.3–5.8 for the mouse Hex B. When crude mouse liver extract was chromatofocused under the same conditions, MUGS-cleaving activity was detected throughout a broader pH range extending from pH 6.5 to 3.8.

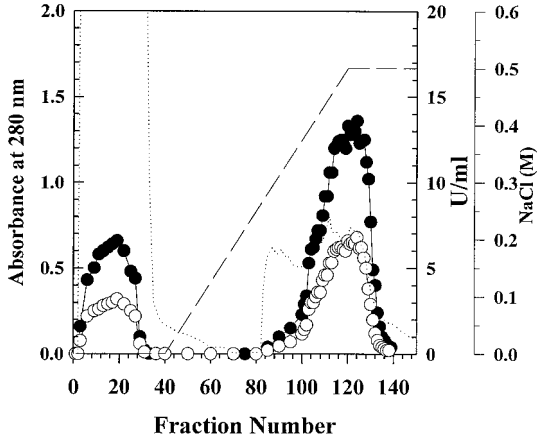

FIG. 3. **SP-Fractogel chromatography of mouse liver Hex A.** Con A-Sepharose purified mouse Hex A was applied onto a SP-Fractogel column (0.5 × 2 cm). Detailed conditions are described under "Experimental Procedures." *Dotted line*, absorbance at 280 nm; *filled circles*, MUG-cleaving activity; *empty circles*, MUGS-cleaving activity; *dashed line*, NaCl gradient.

Using MUG or MUGS in 50 mM sodium citrate buffer, both mouse Hex A and Hex B exhibited maximal activity at pH 5.0. This value is slightly higher than the reported human value of 4.4 (8). The K_m value of Hex A toward MUG and MUGS were 0.98 mM and 0.72 mM, respectively. For Hex B, the K_m value toward MUG was 0.90 mM and toward MUGS was 7.8 mM. Similar values were found for the human isozymes (8, 30, 31).

Expression and Characterization of Mouse G_{M2} Activator—

TABLE I
Purification of Hex A and Hex B from mouse liver

The enzymatic assays and purification were carried out as described under "Experimental Procedures." Steps 1–5 show the preparation of Hex A and steps 1 and 6–9 describe the preparation of Hex B, starting from 200 frozen mouse livers.

Step	Purification	Protein	Total activity	Specific activity	Recovery	Purification
		mg	*units*	*units/mg*	*%*	*-fold*
1	$(NH_4)_2SO_4$, 30–65%, Hex A and B	23010	683.2	0.03	100	1
2	DEAE-Fractogel (adsorbed), Hex A	4454	677.2	0.15	99.1	5
3	Sephacryl S-300-HR, Hex A	3057	841.2	0.28	123	9.3
4	Con A-Sepharose, Hex A	279	813.0	2.91	119	97
5	SP-Fractogel, Hex A	2.8	121.4	43.4	17.8	1447
6	DEAE-Fractogel (non-adsorbed), Hex B	5135	45.8	0.014	100	1
7	SP-Fractogel, Hex B	480	32.8	0.068	71.6	4.6
8	Sephacryl S-300-HR, Hex B	151	22.6	0.150	49.3	10.7
9	Con A-Sepharose, Hex B	0.94	12.9	13.7	28.2	978

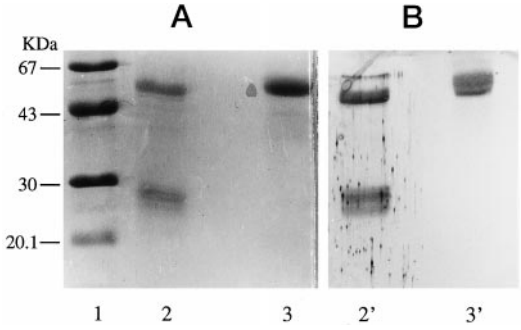

FIG. 4. **Analysis of mouse liver Hex A by SDS-PAGE (*A*) and Western blotting (*B*).** *A*, purified mouse liver Hex A was analyzed by 15% SDS-PAGE according to the conditions described under "Experimental Procedures." Protein bands were visualized by Coomassie Brilliant Blue staining: molecular weight standards (*lane 1*); purified mouse liver Hex A reduced with 2-mercaptoethanol (*lane 2*); purified mouse liver Hex A, not reduced (*lane 3*). *B*, Western blot analysis of purified mouse liver Hex A after 15% SDS-PAGE: purified mouse liver Hex A, reduced with 2-mercaptoethanol (*lane 2*); and purified mouse liver Hex A, not reduced (*lane 3*). Detailed conditions are described under "Experimental Procedures."

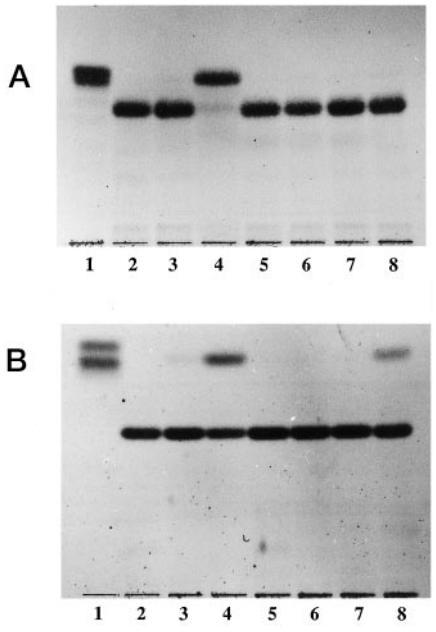

FIG. 5. **Thin layer chromatography showing the hydrolysis of G_{M2} (*A*) and G_{A2} (*B*) by mouse Hex A and Hex B.** The glycolipids (3 nmol) were incubated with 20 milliunits of Hex at 37 °C for 30 min or 6 h for the extended incubation. The detailed assay conditions are described under "Experimental Procedures." The plates were developed with chloroform/methanol/water, 60:35:8 (v/v/v), and stained with diphenylamine reagent. *A*: *1*, G_{M3} standard; *2*, G_{M2} + mouse G_{M2} activator; *3*, G_{M2} + mouse Hex A; *4*, G_{M2} + mouse Hex A + mouse G_{M2} activator; *5*, G_{M2} + mouse Hex B; *6*, G_{M2} + mouse Hex B + mouse G_{M2} activator; *7*, G_{M2} + mouse Hex B, 6 h of incubation; *8*, G_{M2} + mouse Hex B + mouse G_{M2} activator, 6 h of incubation. *B*: *1*, LacCer; *2*, G_{A2} + mouse G_{M2} activator; *3*, G_{A2} + mouse Hex A; *4*, G_{A2} + mouse Hex A + mouse G_{M2} activator; *5*, G_{A2} + mouse Hex B; *6*, G_{A2} + mouse Hex B + mouse G_{M2} activator; *7*, G_{A2} + mouse Hex B, 6 h of incubation; *8*, G_{A2} + mouse Hex B + mouse G_{M2} activator, 6 h of incubation.

The molecular mass of the recombinant mouse G_{M2} activator determined by SDS-PAGE was 18.5 kDa, which is as expected from the cDNA sequence and is identical to that of the human G_{M2} activator. By Western blot analysis, mouse G_{M2} activator was recognized by the polyclonal antibodies against human G_{M2} activator, indicating similarities in protein structure, although with a weaker interaction than that for the human G_{M2} activator.

Hydrolysis of G_{M2} by Mouse Hex A and Hex B—The purified mouse Hex A and Hex B were examined for their ability to hydrolyze G_{M2}. As shown in Fig. 5*A*, the specificities of the mouse Hex A and Hex B toward G_{M2} are the same as their human counterparts. Under the same conditions, mouse Hex A effectively hydrolyzes G_{M2} but only in the presence of the mouse G_{M2} activator (Fig. 5*A*, *lane 4*, 88% hydrolysis). Similar to human Hex B, but in contrast to the previous report (3), mouse Hex B is not able to cleave G_{M2} in the absence of G_{M2} activator (Fig. 5*A*, *lane 5*) even after extended incubation (Fig. 5*A*, *lane 7*). While in the presence of G_{M2} activator, only a very trace of G_{M3} production by mouse Hex B is detected after 30 min of incubation (Fig. 5*A*, *lane 6*) or 6 h of incubation (Fig. 5*A*, *lane 8*). These results clearly indicate that mouse Hex B is similar to human Hex B with regard to the specificity for G_{M2} hydrolysis.

Hydrolysis of G_{A2} by Mouse Hex A and Hex B—To understand the reported observations on the studies of mouse Hex α-chain disruption (12, 13), we also examined the ability of two mouse Hex isozymes to hydrolyze the GalNAc from G_{A2} (Fig. 5*B*). Under our assay conditions (30 min of incubation), mouse Hex A was found to slowly hydrolyze G_{A2} in the absence of mouse G_{M2} activator (Fig. 5*B*, *lane 3*). We found that even though G_{A2} is refractory to human Hex A in the presence of human G_{M2} activator (19), mouse Hex A was able to effectively hydrolyze G_{A2} in the presence of mouse G_{M2} activator (Fig. 5*B*, *lane 4*, 45% hydrolysis). Under the same conditions, mouse Hex B was not able to hydrolyze G_{A2} in the absence of mouse G_{M2} activator (Fig. 5*B*, *lane 5*), and no detectable hydrolysis was observed in the presence of mouse G_{M2} activator (Fig. 5*B*, *lane 6*) after 30 min of incubation. However, after extended incubation (6 h of incubation), mouse Hex B was found to be able to slowly hydrolyze G_{A2} in the presence of mouse G_{M2} activator (Fig. 5*B*, *lane 8*).

It has been shown previously that the ceramide portion of the

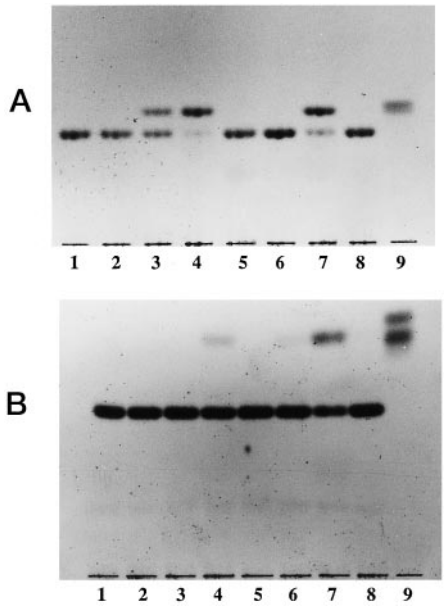

FIG. 6. **Species specificity of human and mouse G_{M2} activators toward the hydrolysis of G_{M2} (*A*) and G_{A2} (*B*) by human and mouse Hex A.** Each glycolipid substrate (3 nmol) was incubated with 20 milliunits of Hex at 37 °C for 30 min. The plates were developed with chloroform/methanol/water, 60:35:8 (v/v/v), and stained with diphenylamine reagent. The detailed assay conditions are described under "Experimental Procedures." *A*: *1*, G_{M2} + human G_{M2} activator; *2*, G_{M2} + human Hex A; *3*, G_{M2} + human Hex A + human G_{M2} activator; *4*, G_{M2} + human Hex A + mouse G_{M2} activator; *5*, G_{M2} + mouse G_{M2} activator; *6*, G_{M2} + mouse Hex A; *7*, G_{M2} + mouse Hex A + mouse G_{M2} activator; *8*, G_{M2} + mouse Hex A + human G_{M2} activator; *9*, G_{M3}. *B*: *1*, G_{A2} + human G_{M2} activator; *2*, G_{A2} + human Hex A; *3*, G_{A2} + human Hex A + human G_{M2} activator; *4*, G_{A2} + human Hex A + mouse G_{M2} activator; *5*, G_{A2} + mouse G_{M2} activator; *6*, G_{A2} + mouse Hex A; *7*, G_{A2} + mouse Hex A + mouse G_{M2} activator; *8*, G_{A2} + mouse Hex A + human G_{M2} activator; *9*, LacCer.

G_{M2} molecule is essential for hydrolysis by human Hex A (10, 19). As is the case for the human enzyme, neither mouse Hex isozyme was able to hydrolyze $II^3NeuAcGgOse_3$, the oligosaccharide derived from G_{M2}, even in the presence of G_{M2} activator (data not shown).

The mouse Hex A and Hex B are highly homologous to their human counterparts, with the α- and β-chains sharing 85 and 74% identity, respectively, at the amino acid level (26–28). The mouse G_{M2} activator is also quite similar to the human protein, sharing 75% identity (18). Therefore, we studied the ability of human and mouse activators to cross-stimulate G_{M2} and G_{A2} hydrolysis by human and mouse Hex A. Using the same units (20 milliunits) of human and mouse Hex A and the same amount (1 μg) of human and mouse G_{M2} activator, we found that the mouse activator effectively stimulated the hydrolysis of G_{M2} by both human Hex A (Fig. 6*A*, *lane 4,* 83% hydrolysis) and mouse Hex A (Fig. 6*A*, *lane 7,* 72% hydrolysis). It appears that the mouse G_{M2} activator is more effective in stimulating the hydrolysis of G_{M2} by human Hex A. Under the same conditions, the human G_{M2} activator stimulated only 57% hydrolysis of G_{M2} by human Hex A (Fig. 6*A*, *lane 3*). The human G_{M2} activator was also much less effective in stimulating the hydrolysis of G_{M2} by mouse Hex A (Fig. 6*A*, *lane 8*), which could be seen after extended incubation or in the presence of additional activator protein (data not shown). Of great interest was the observation that the mouse G_{M2} activator also stimulated the hydrolysis of G_{A2} by human Hex A (Fig. 6*B*, *lane 4*). In contrast, the human activator was not able to promote the hydrolysis of G_{A2} by human Hex A (Fig. 6*B*, *lane 3*) or mouse Hex A (Fig. 6*B*, *lane 8*). Extended incubation of the mouse activator with human Hex B resulted in the slow hydrolysis of G_{A2} (data not shown) as seen for mouse activator with mouse Hex B (Fig. 5*B*, *lane 8*).

DISCUSSION

To understand the catabolism of G_{M2} in mouse, we have purified and characterized mouse liver Hex A and Hex B and compared their properties with human Hex A and Hex B. As seen with the recombinantly expressed α- and β-chains (25), the purified mouse liver Hex A was recognized by goat anti-human Hex A. Purified mouse Hex A was determined to be composed of 57- and 59-kDa subunits by SDS-PAGE under nonreducing conditions, and smaller polypeptides were observed in the presence of 2-mercaptoethanol or dithiothreitol (Fig. 4*A, lane 2*). Therefore, mouse Hex A has a similar subunit composition to human Hex A, with noncovalently linked α- and β-subunits (2). This is also the first direct evidence that one of the subunits is composed of nonidentical cystine-linked polypeptide chains, which, by comparison with the human enzyme, is probably the β-subunit (29).

While the isoelectric points of purified mouse Hex A and Hex B are similar to the isoelectric points of their human counterparts, the presence of mouse Hex A distributed in a wide range of isoelectric points has important consequences for purification. In the past, the separation of the mouse Hex A and Hex B isozymes has been routinely accomplished by passing a preparation over an anion exchange column equilibrated with 10 mM sodium phosphate buffer, pH 6.0–6.5. Hex B is collected in the pass-through fractions, while the retained Hex A is eluted by an NaCl gradient (3, 32). However, these reports followed the method that was originally optimized for the human Hex isozymes (1). We found that in following the previously reported methods (3), the mouse Hex B preparation that was not adsorbed to the DEAE column at pH 6.0–6.5 still contained a small amount of MUGS-cleaving activity. MUGS-cleaving activity has been correlated with the ability to hydrolyze G_{M2} (33). As reported by Burg *et al.* (3), we also found that mouse Hex B prepared by this method did contain some G_{M2}-cleaving activity. To ascertain whether this G_{M2}-cleaving activity was inherent in the mouse Hex B or due to contamination by Hex A, we increased the pH of the buffer solution to 7.0 for the separation of the two isozymes by anion exchange chromatography. Interestingly, the amount of MUGS-cleaving activity, as compared with the MUG-cleaving activity, decreased significantly and the resulting Hex B preparation became extremely weak in hydrolyzing G_{M2} (Fig. 5*A*), as was observed with human Hex B (11).

From the binding behavior of mouse Hex A to DEAE-Fractogel and also because of its acidic pI, the retention of the enzyme by the SP-Fractogel column at pH 7.0 (Fig. 3) was totally unexpected. This suggests that interactions other than ionic may be involved. This chromatography step was very effective for removing contaminating proteins. Because the Hex B preparation contained other proteins not adsorbed to DEAE-Fractogel at pH 7.0, it is not surprising that the SP-Fractogel chromatography was not as effective for purifying Hex B as for Hex A. Based on the DEAE-Fractogel chromatography, we estimated that approximately 90% of the total MUG-cleaving activity present in the crude mouse liver extract was Hex A and 7% was Hex B. This is in agreement with previous reports of the level of the two isozymes in mouse liver tissues (32). Because the amount of Hex B in mouse liver is very low compared with Hex A it was not practical to purify Hex B to homogeneity as done for Hex A. However, the final Hex B preparation is free from contaminating glycosidases and proved to be suitable for the studies presented.

The recombinant human and mouse G_{M2} activators were expressed using the shortened version of cDNAs which encode

only the mature activator proteins. The cDNA for human G_{M2} activator encodes for a protein of 193 amino acids that consists of a signal peptide (23 amino acids), a propeptide (8 amino acids), and a mature protein (162 amino acids). The signal and the propeptides are excised proteolytically to form the mature G_{M2} activator protein (5). In the full-length cDNA encoding for the mouse G_{M2} activator, the predicted cleavage site is between positions 19 and 20 of the deduced amino acid sequence (34). This site is very close to the cleavage site (positions 23 and 24) of the human sequence (5). Although there is no direct evidence that the first 31 amino acids in the mouse sequence contains a signal peptide and a propeptide, the mouse sequence shows a hydropathy profile similar to that of the human sequence (18). In addition, the recombinant mouse G_{M2} activator and the native human protein were found to have the same specific activity toward the hydrolysis of G_{M2}, indicating that the mature form of mouse G_{M2} activator is very likely to start from amino acid 32 as in the case of humans.

As seen with the human Hex isozymes, mouse Hex A hydrolyzes G_{M2}, with the requirement of the G_{M2} activator, whereas mouse Hex B has only a trace of activity to cleave G_{M2} with or without G_{M2} activator. To our surprise, in contrast to human Hex isozymes, mouse Hex A was also able to effectively hydrolyze G_{A2} in the presence of mouse G_{M2} activator (Fig. 5*B*, *lane 4*). We were not able to detect the hydrolysis of G_{A2} by Hex B without G_{M2} activator, but when the activator is present, some hydrolysis of G_{A2} could be seen after extended incubation (Fig. 5*B, lane 6*). These results provide the explanation for the observations made in mice with disrupted α-subunit gene. Mice defective in Hex A but not Hex B, because of the disrupted α-subunit were found to show relatively little buildup of G_{M2} or G_{A2} with no behavioral abnormalities, as compared with humans with defective α-subunits. (12, 13). The fact that mouse Hex B cannot hydrolyze G_{M2} but can act on G_{A2} suggests that in mice G_{M2} can be converted to G_{A2} that serves as a substrate for mouse Hex B. We have shown previously that clostridial sialidase can effectively convert G_{M2} to G_{A2} in the presence of human G_{M2} activator (35). Our results complement the recent pathobiological findings of the three mouse models of human Tay-Sachs disease, types B, O, and AB of G_{M2} gangliosidosis. The mouse models of type B (*Hexa*$-/-$) and O (*Hexb*$-/-$) were generated by targeted disruption of Hex A (α-subunit) (12, 13) or Hex B (subunit) (36) genes encoding Hex A ($\alpha\beta$) and Hex B ($\beta\beta$). The model of type AB G_{M2} gangliosidosis (*Gm2a* $-/-$) (G_{M2} activator deficiency) was produced by targeted disruption of *Gm2a* gene (37). Unlike human type B G_{M2} gangliosidosis, the *Hexa* $-/-$ mice were asymptomatic (12, 13), while *Hexb* $-/-$ mice (36) were severely affected as in the case of human type O G_{M2} gangliosidosis. The *Hexb* $-/-$ mice accumulated more G_{M2} and G_{A2} in the brain than the *Hexa* $-/-$ mice. The *Gm2a* $-/-$ mice (37) showed a phenotype which is intermediate to those of *Hexa* $-/-$ (12, 13) and *Hexb* $-/-$ (36) with storage of an excess amount of G_{M2} and a low amount of G_{A2}. From these three murine models of Tay-Sachs disease, it has been proposed that *Hexa* $-/-$ mice escape the disease through partial catabolism of G_{M2} via G_{A2} by the combined action of sialidase and Hex B (14). The pathogenesis of *Gm2a* $-/-$ mice also suggested a role for the G_{M2} activator in G_{A2} degradation in mice (37).

Our results provide the explanation for the results generated by the above three mouse models. We have demonstrated the ability of mouse Hex A to participate in the catabolism of G_{A2} and a very weak activity of Hex B toward the degradation of G_{M2}. We have also shown the ability of mouse G_{M2} activator to stimulate the hydrolysis of G_{A2} by mouse Hex A and to a lesser extent by mouse Hex B. We have also examined the species specificity of the interactions between the mouse and human Hex isozymes and the activators. Previously, crude activator preparations from other mammalian species (3) and purified mullet roe G_{M2} activator (38) were found to activate the hydrolysis of G_{M2} by human Hex A. We have shown here that purified recombinant mouse G_{M2} activator can effectively stimulate the hydrolysis of G_{M2} and G_{A2} by human Hex A. In reverse, human G_{M2} activator was not effective in stimulating the hydrolysis of G_{M2} or G_{A2} by mouse Hex A.

Although the mouse G_{M2} activator is 73.5% identical to the human protein, it also appears that the mouse activator does not share the specificity to the characteristic branched trisaccharide epitope of G_{M2} (19) but assists Hex A to hydrolyze G_{A2} as well. The observation that mouse G_{M2} activator can stimulate the hydrolysis of G_{M2} by both human and mouse Hex A, while human G_{M2} activator can only stimulate the hydrolysis of G_{M2} by human Hex A but not mouse Hex A, provides strong evidence that the G_{M2} activator proteins must somehow interact with Hex A. Similarly, the observation that the mouse G_{M2} activator can stimulate the hydrolysis of both G_{M2} and G_{A2} by human Hex A, but the human G_{M2} activator can only stimulate the hydrolysis of G_{M2} by human Hex A, shows that the G_{M2} activators of these two species may have different specificities for the two glycolipids.

Biochemical analysis of enzyme systems is an important complement to molecular and genetic studies in the effort to fully understand the roles of Hex isozymes in mouse. Despite the biochemical similarities between human and mouse Hex isozymes and G_{M2} activator proteins, the catabolic pathways for G_{M2} in mouse and human are clearly not identical. Therefore, the murine model for Type B Tay-Sachs disease does not truly reflect its counterpart in man.

REFERENCES

1. Robinson, D., and Stirling, J. L. (1968) *Biochem. J.* **107,** 321–327
2. Geiger, B., and Arnon, R. (1976) *Biochemistry* **15,** 3484–3493
3. Burg, J., Banerjee, A., Conzelmann, E., and Sandhoff, K. (1983) *Hoppe-Seyler's Z. Physiol. Chem.* **364,** 821–829
4. Li, Y.-T., and Li, S.-C. (1984) in *Lysosomes in Biology and Pathology* (Dingle, J. T., Dean, R. T., and Sly, W.. eds.) pp. 99–117, Elsevier Science Publishers B. V., Amsterdam
5. Fürst, W., and Sandhoff, K. (1992) *Biochim. Biophys. Acta* **1126,** 1–16
6. Kishimoto, Y., Hiraiwa, M., and O'Brien, J. S. (1992) *J. Lipid Res.* **33,** 1255–1267
7. Sandhoff, K., and Wassle, W. (1971) *Z. Physiol. Chem.* **352,** 1119–1133
8. Wenger, D. A., Okada, S., and O'Brien, J. S. (1972) *Arch. Biochem. Biophys.* **153,** 116–129
9. Li, Y.-T., Mazzotta, M. Y., Wan, C.-C., Orth, R., and Li, S.-C. (1973) *J. Biol. Chem.* **248,** 7512–7515
10. Li, S.-C., Hirabayashi, Y., and Li, Y.-T. (1981) *J. Biol. Chem.* **256,** 6234–6240
11. Gravel, R. A., Clarke, J. T. R., Kaback, M. M., Mahuran, D., Sandhoff, K., and Suzuki, K. (1995) in *The Metabolic and Molecular Basis of Inherited Disease* (Scriver, C. V., Beaudet, A. L., Sly, W. S., and Valle, D., eds.) pp. 2839–2879, McGraw-Hill, New York
12. Yamanaka, S., Johnson, M. D., Grinberg, A., Westphal, H., Crawley, J. N., Taniike, M., Suzuki, K., and Proia, R. L. (1994) *Proc. Natl. Acad. Sci. U. S. A.* **91,** 9975–9979
13. Cohen-Tannoudji, M., Marchand, P., Akli, S., Sheardown, S. A., Puech, J.-P., Kress, C., Gressens, P., Nassogne, M.-C., Beccari, T., Muggleton-Harris, A. L., Evrard, P., Stirling, J. L., Poenaru, L., and Babinet, C. (1995) *Mamm. Genome* **6,** 844–849
14. Sango, K., Yamanaka, S., Hoffmann, A., Okuda, Y., Grinberg, A., Westphal, H., McDonald, M. P., Crawley, J. N., Sandhoff, K., Suzuki, K., and Proia, R. L. (1995) *Nat. Genet.* **11,** 170–176
15. Svennerholm, L. (1972) *Methods Carbohydr. Chem.* **6,** 464–474
16. Svennerholm, L., Månsson, J.-E., and Li, Y.-T. (1973) *J. Biol. Chem.* **248,** 740–742
17. Zhou, B., Li, S.-C., Laine, R. A., Huang, R. T. C., and Li, Y.-T. (1989) *J. Biol. Chem.* **264,** 12272–12277
18. Bellachioma, G., Stirling, J. L., Orlacchio, A., and Beccari, T. (1993) *Biochem. J.* **294,** 227–230
19. Wu, Y. Y., Lockyer, J. M., Sugiyama, E., Pavlova, N. V., Li, Y.-T., and Li, S.-C. (1994) *J. Biol. Chem.* **269,** 16276–16283
20. Potier, M., Mameli, L., Bélisle, M., Dallaire, L., and Melançon, S. B. (1979) *Anal. Biochem.* **94,** 287–296
21. Harris, G., and MacWilliams, I. C. (1954) *Chem. Ind. (London),* 249
22. Yuziuk, J. A., Nakagawa, H., Hasegawa, A., Kiso, M., Li, S.-C., and Li, Y.-T. (1996) *Biochem. J.* **315,** 1041–1048
23. Laemmli, U. K. (1970) *Nature* **227,** 680–685
24. Hasilik, A., and Neufeld, E. F. (1980) *J. Biol. Chem.* **255,** 4937–4945
25. Pennybacker, M., Liessem, B., Moczall, H., Tifft, C. J., Sandhoff, K., and Proia, R. L. (1996) *J. Biol. Chem.* **271,** 17377–17382

26. Beccari, T., Hoade, J., Orlacchio, A., and Stirling, J. L. (1992) *Biochem. J.* **285,** 593–596
27. Yamanaka, S., Johnson, O. N., Norflus, F., Boles, D. J., and Proia, R. L. (1994) *Genomics* **21,** 588–596
28. Bapat, B., Ethier, M., Neote, K., Mahuran, D., and Gravel, R. A. (1988) *FEBS Lett.* **237,** 191–195
29. O'Dowd, B. F., Cumming, D. A., Gravel, R. A., and Mahuran, D. (1988) *Biochemistry* **27,** 5216–5226
30. Inui, K., and Wenger, D. A. (1984) *Clin. Genet.* **26,** 318–321
31. Bayleran, J., Hechtman, P., Kolodny, E., and Kaback, M. (1987) *Am. J. Hum. Genet.* **41,** 532–548
32. Beccari, T., Orlacchio, A., and Stirling, J. L. (1988) *Biochem. J.* **252,** 617–620
33. Fuchs, W., Navon, R., Kaback, M., and Kresse, H. (1983) *Clin. Chim. Acta* **133,** 253–261
34. Nielsen, H., Engelbrecht, J., Brunak, S., and Von Heijne, G. (1997) *Protein Eng.* **10,** 1–6
35. Li, S.-C., Wu, Y.-Y., Sugiyama, E., Taki, T., Kasama, T., Casellato, R., Sonnino, S., and Li, Y.-T. (1995) *J. Biol. Chem.* **270,** 24246–24251
36. Paneuf, F., Wakamatsu, N., Huang, A., Peterson, A. C., Fortunato, S. R., Ritter, G., Igdoura, S. A., Morales, C. R., Benoit, G., Akerman, B. R., Leclerc, D., Hanai, N., Marth, J. D., Trasler, J. M., and Gravel, R. A. (1996) *Hum. Mol. Genet.* **5,** 1–14
37. Liu, Y., Hoffmann, A., Grinberg, A., Westphal, H., McDonald, M. P., Miller, K. M., Crawley, J. N., Sandhoff K., Suzuki, K., and Proia, R. (1997) *Proc. Natl. Acad. Sci. U. S. A.* **94,** 8138–8143
38. DeGasperi, R., Li, Y.-T., and Li, S.-C. (1989) *Biochem. J.* **260,** 777–783

Specificity of Mouse G_{M2} Activator Protein and β-*N*-Acetylhexosaminidases A and B: SIMILARITIES AND DIFFERENCES WITH THEIR HUMAN COUNTERPARTS IN THE CATABOLISM OF GM2

Jeffrey A. Yuziuk, Carmen Bertoni, Tommaso Beccari, Aldo Orlacchio, Yan-Yun Wu, Su-Chen Li and Yu-Teh Li

J. Biol. Chem. 1998, 273:66-72.
doi: 10.1074/jbc.273.1.66